TRACING WADDEN SEA WATER MASSES WITH AN INVERSE BIO-OPTICAL AND ENDMEMBER MODEL

Annelies Hommersom[1], Steef Peters[1], Hendrik Jan van der Woerd[1], Marieke A. Eleveld[1], Marcel R. Wernand[2] and Jacob de Boer[1]

1. Institute for Environmental Studies (IVM), VU University, De Boelelaan 1085, 1081 HV Amsterdam, The Netherlands; annelies.hommersom@gmail.com, {steef.peters / hans.van.der.woerd / marieke.eleveld / jacob.de.boer}(at)ivm.vu.nl
2. Royal Netherlands Institute for Sea Research (NIOZ), P.O. Box 59, 1790 AB Den Burg (Texel), The Netherlands; wernand(at)nioz.nl

ABSTRACT

With its 500 km length the Wadden Sea is the largest mudflat area in the world. Discharges from various rivers mix here with water from the North Sea. Due to surfacing tidal flats during low tide, the variation in source water, resuspension and extremely high concentrations of Chlorophyll-a (Chl-a), Suspended Particulate Matter (SPM), and Coloured Dissolved Organic Matter (CDOM), large temporal and spatial differences in watercolour can be seen.

To visualise the horizontal mixing of water masses with different colours from MERIS data, two approaches were followed. The first approach was an inverse bio-optical model called HYDROPT, in which the absorption and scattering properties of the water constituents (Specific Inherent Optical Properties or SIOPs) can be adapted to regional values. This approach can be used to determine “water types”: water masses in which the SIOPs of the constituents are similar. The second approach was an endmember model, based on spectral reflectance shapes. This approach can be used to determine “water classes”: water types in which certain constituents are predominant. The predicted water types and water classes were compared with knowledge on (tidal) distributions of water types in the Wadden Sea.

In the data of March ’07 (winter) and May ’06 (summer) differences in water types between the North Sea, the Wadden Sea and water originating from the large rivers were seen in the German Bight. The endmember approach was able to visualise mixing between water classes. Results of this method showed dominance by SPM in winter and much higher concentrations of Chl-a and CDOM in summer. A combination of the two methods would probably lead to the best tracing of water masses.

INTRODUCTION

Remote sensing of estuaries and tidal flat areas is complex due to the often extreme turbidity and heterogeneity, and explores therefore the upper limits of knowledge on remote sensing of coastal zones. Remote sensing in these areas requires algorithms tuned for the extremely high concentrations of various substances, almost simultaneous acquisition of remote sensing data and *in situ* data for validation because of the fast changes as a result of resuspension due to tidal currents, and local knowledge of optical properties to tune the algorithm. Apart from these problems, remote sensing of coastal zones is an interesting possibility to water quality monitoring programmes. The new Water Framework Directive regulations from the European Union expect the member states to monitor all their coastal areas (1). Monitoring is important to maintain the ecological and economical values of coastal zones, which are at the same time the most densely populated areas in the world. Monitoring these coastal waters by ship is, as far as possible, a costly and time consuming activity, where remote sensing can offer an alternative. The great advantage of spaceborne remote sensing data is its high spatial resolution combined with a relatively high temporal resolution. The drawback is that some, but not all substances important for water quality can directly be monitored

with spaceborne remote sensing data (2). However, many water quality parameters (such as nutrients) can indirectly be related to parameters that can be detected with remote sensing (3,2).

The Wadden Sea is a very turbid and optically heterogeneous area. It is an embayment where the estuary of various rivers (Rhine via Lake IJssel, Ems, Jade, Weser, Elbe) and North Sea water confluence (Figure 1). The Wadden Sea is the largest tidal flat area in the world. The extreme near-surface concentrations of Particulate Suspended Matter (SPM: 5- 450 g m^{-3}), chlorophyll-a (Chl-a: 1-50 mg m^{-3}), Coloured Dissolved Organic Matter (CDOM: 0.1-3 m^{-1}), and the spatial, tidal and seasonal variations (4) make the Wadden Sea optically very complex and a good case study area for remote sensing in extremely turbid areas. The objectives of this study are therefore to examine to what extent detection of water masses is possible in the Wadden Sea using MERIS data. The possibilities of optical water mass detection based on ternary plots (in which the total absorption was distributed over the relative absorption by Chl-a, SPM and CDOM) were proven by Arnone, Gould and others (e.g., 5,6). In this study we compare a regionally calibrated inverse bio-optical model and an endmember model.

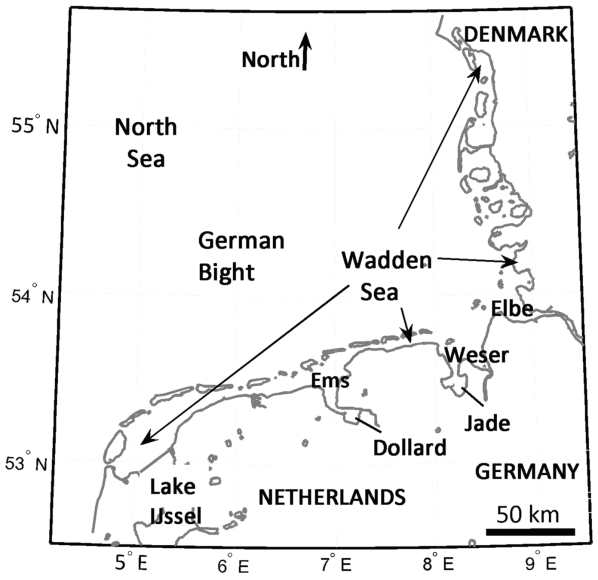

Figure 1. The Wadden Sea.

The inverse bio-optical model, called HYDROPT (7), facilitates the input of different (regional) sets of Specific Inherent Optical Properties of water constituents (SIOPs). The model can automatically select a set of SIOPs from a given list that leads to the best modelled reflectance spectrum compared to the measured spectrum. Its output includes the used SIOP set. This approach can therefore be used to determine water masses in which the SIOPs of the constituents are similar (8), called “water types” here. The second approach was an endmember model, based on spectral reflectance shapes. The model unmixes the measured spectrum in a combination of predefined extreme spectra, called endmembers. This approach can therefore be used to determine water masses in which certain constituents are predominant, called “water classes” here. The predicted water types and water classes are compared with the knowledge on (tidal) distributions of water masses in the Wadden Sea.

METHODS

Satellite data

MERIS data L1 FR reflectance spectra (IPF 5.05/MEGS7.4, ESA, 2009) were pre-processed in the Basis ERS & ENVISAT (A)ATSR and MERIS (BEAM) Toolbox. Adjacency effects were reduced with the “improve contrast between ocean and land” (ICOL) processor (9). Next, the data was atmospherically corrected with the Case-2 regional (C2R) processor (10).

The ICOL and C2R algorithms have their own land, cloud and quality flags (9,11). To be sure only water pixels were processed, the standard C2R land flag was reduced to "toa_reflec_10 > toa_reflec_6", flagging more pixels at shallow locations than the original expression. Since clouds were sometimes flagged as "land" by C2R, the L1 flag for clouds was applied. Data flagged with the C2R flags (RAD_ERR, TOSA_OOR, WLR_OOR and ATC_OOR) were flagged as "flagged input" and not processed with HYDROPT or the endmember model.

Data of two acquisitions were chosen to trace water types and water classes: the data of March 12th 2007, representing a "winter" or before-bloom situation, and the data of July 4th 2006, representing a summer situation. The open North Sea is masked, because the SIOP sets used in HYDROPT were all measured in or just outside the Wadden Sea and were therefore not supposed to be suitable for the open North Sea.

Inverse bio-optical model HYDROPT

HYDROPT is an inverse bio-optical model: it calculates the IOPs, absorption (*a*) and scattering (*b*), from a given reflectance spectrum. HYDROPT includes a lookup table (LUT) based on HydroLight (12) simulations of reflectances as a function of IOPs. Reflectances per wavelength over a large range of *a* and *b* are included. The model was calibrated for each run with one or more sets of Specific Optical Properties (SIOPs) at MERIS wavelengths. The absorption and scattering values at the correct solar angle and viewing geometry in the LUT can be constructed from these SIOP sets plus concentrations of Chl-a, SPM, and CDOM via Eqs. (1) and (2).

$$a(\lambda) = a_w(\lambda) + a^*_{chl}(\lambda)\cdot[Chl-a] + a^*_{SPM}(\lambda)\cdot[SPM] + a^*_{CDOM}(\lambda)\cdot a_{CDOM}(440) \quad (1)$$

$$b(\lambda) = b_w(\lambda) + b^*_{SPM}(\lambda)\cdot[SPM] = b_w(\lambda) + \frac{b^*_{b,SPM}(\lambda)}{B(\lambda)}\cdot[SPM] \quad (2)$$

a_w is the total absorption of water, a^*_{chl}, a^*_{SPM} and a^*_{CDOM} are the specific absorption coefficients for respective pigments, particles other than phytoplankton, and *CDOM*. [*Chl-a*] and [*SPM*] are the concentrations of *Chl-a* and *SPM*. For *CDOM*, the value at 440 nm is taken to normalise the attenuation (a_{CDOM}). b_w is the scattering coefficient for water, b^*_{SPM} is the specific scattering coefficient and $b^*_{b,SPM}$ the specific backscattering coefficient for *SPM*. *B* is the backscattering to scattering ratio, which was assumed to be spectrally neutral 0.03 (13-16). For each given reflectance spectrum, HYDROPT finds a reflectance spectrum from the LUT based on the entered SIOP sets and values for [*Chl-a*], [*SPM*] and a_{CDOM}. In the optimisation, the modelled spectrum is compared to the measured spectrum with a least-squares criterion of the band differences, Eq. (3). In Eq. (3), *Rrs* is the remote sensing reflectance, *i* is the band number and σ is the estimated standard error in the band differences, which was arbitrarily set to $3E^{-4}$ and *m* is *i*-1. In this study σ was given the same value for TriOS and MERIS data.

$$\chi^2 = \sum_1^m \left[\frac{(Rrs_{(i+1)} in\ situ - R_i\ in\ situ) - (Rrs_{(i+1)}\ modelled - Rrs_i\ modelled)}{\sigma} \right]^2 \quad (3)$$

HYDROPT optimises the spectral fit by varying [*Chl-a*], [*SPM*] and a_{CDOM} and the SIOP sets. Subsequently the outputs are: the spectrum that was chosen from the LUT, χ^2, [*Chl-a*], [*SPM*], a_{CDOM}, confidence intervals of these concentrations and the used SIOP set. Water for which the same SIOP set leads to the best fitting spectrum is defined as one water type. Therefore, the maximum possible number of traced water types is the number of SIOP sets the model is calibrated with.

At *in situ* campaigns in 2006 and 2007 *[Chl-a]*, *[SPM]*, a_{CDOM} were measured, a^*_{Chl}, a^*_{SPM} were derived directly from filter pad measurements in 2007, while b^*_{SPM} was calculated from the measured beam attenuation and the measured absorptions (3). The i*n situ* reflectance was calculated from above-water radiance and irradiance measurements measured with TriOS sensors (3). Due to equipment failure the accuracy of the CDOM measurements in 2007 was lost, instead, a^*_{CDOM} derived from measurements at almost the same locations in 2006 was used in the SIOP sets.

Initial runs showed that water type detection in MERIS data was only possible when band 412 nm was omitted from the analysis, probably due to the relatively large noise level in this band (17). Using 7 bands, χ^2 values ≤7.81 (3 degrees of freedom, P=0.05) were defined as a good spectral fit. The most representative SIOP sets were selected by providing HYDROPT with a list of 22 SIOP sets as measured at *in situ* stations (3) and performing runs with 135 TriOS spectra as input (Figure 2). HYDROPT selected four SIOP sets for >80% of the TriOS measurements (Table 2). These SIOP sets were considered to be most representative and were used for water type detection on MERIS data (Figure 2). For each pixel HYDROPT selected one of the four SIOP sets to model the spectrum. The pixels for which the same SIOP set was chosen are mapped to show the distribution of water types.

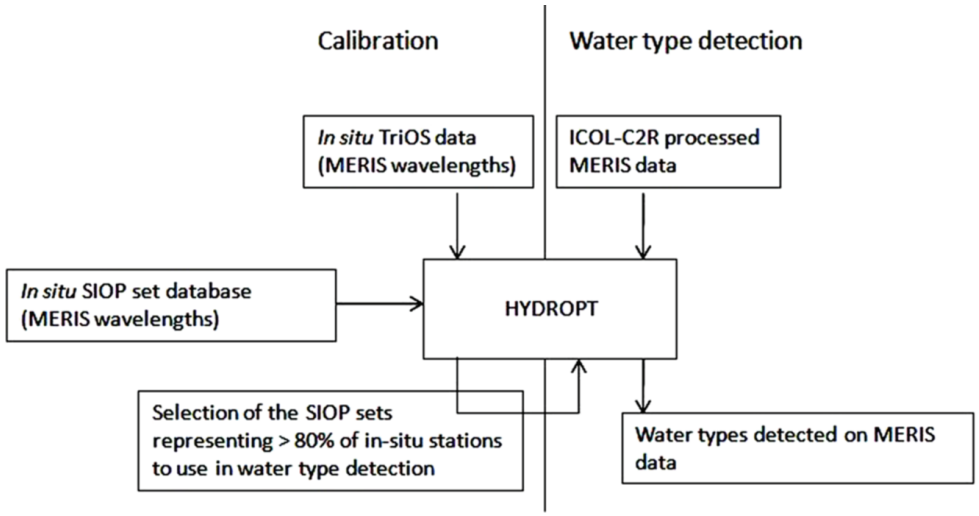

Figure 2. Diagram of the water type detection with HYDROPT.

Table 1. SIOP sets selected for water type detection. Absorption of CDOM was not measured simultaneously with a^*_{Chl} and a^*_{SPM}, other properties are given as measured simultaneously with a^*_{Chl} and a^*_{SPM}.

SIOP set	**1**	**2**	**3**	**4**
in-situ location	Wadden Sea	North Sea	Ems estuary	Wadden Sea
Tide	ingoing	almost high	almost high	outgoing
salinity (Practical Salinity Scale)	32	32	25	33
organic content (%)	15.7	27.1	26.2	not available
a^*_{Chl} (681 nm) (m^{-2} mg^{-1})	0.80E-2	0.83E-2	1.65E-2	18.4E-2
a^*_{SPM} (442 nm) (m^{-2} g^{-1})	1.81E-2	2.89E-2	14.14E-2	1.91E-2
a_{CDOM}(442 nm) (m^{-1})	0.978	0.972	0.953	0.961

Endmember model

Endmember methods are common in land-remote sensing, but almost new to water remote sensing (18), where endmember abundances have been used by few researchers, for deriving Chl-a concentrations (19,20) and local calibration (21), not yet for tracing of water masses. For land cover applications these methods are often used to determine abundances of ground coverage of certain types within a pixel, in cases where typical ground coverages are well known, while their spatial distribution contains too many entities smaller than the pixel size. An example is grassland with asphalted roads through it. Generally, the roads will be too small to be separately seen in the satellite data, while all pixels contain a mixture of light reflected by grass and asphalt. Endmember methods use spectra of the most extreme situations occurring, e.g. pure grass reflectance and pure asphalt reflectance, called “endmembers”, to unmix a measured spectrum. Linear unmixing uses Eq. (4), in which R_1 to R_n are the endmembers and *a-i* the coefficients, or abundances of the endmembers, determined in the unmixing process. Following the example, the calculated abun-

dances will provide the percentage coverage by grass and road per pixel. As will be explained later, in our model n = 9.

$$R_{measured} = aR_1 + bR_2 + cR_3 + \ldots + iR_n \quad (4)$$

There are several ways to define the spectra to be used as endmembers, for example:

- Knowledge based manual selection. This method is fast and easy, however, not objective.
- Pure pixel approach. In this approach spectra of all pixels are placed in a coordinate system with a wavelength on both axes. This is repeated with other wavelengths and the spectra that occur most often at the outer places of the scatter plots are selected as endmembers. This method is objective, however, in sea (almost) no pure spectra can be found and endmembers will vary per acquisition due to variation in optical properties over the season.
- Statistical classification, for example with *K*-means, selecting the class means. This method is objective; however, although these endmembers will represent water types, they will not represent the extremes.
- Simulation of "pure" spectra. This method is fairly objective, however, simulations require a model and modelling always implies prepositions about, for example, inherent optical properties of an area, or shapes of apparent optical properties. Therefore, endmembers generated for a certain region can be less suitable in other regions.

In this experiment endmembers were generated via the last approach. The Gordon (22,23) model, Eq. (5), was used in combination with Eqs. (2) and (3), the assumption f = 0.33 (24) and the median SIOP values as measured in the Wadden Sea needed for Eqs. (2) and (3).

$$Rrs = 1.33^2 \pi \left(\frac{f \cdot b_b}{a + b_b} \right) \quad (5)$$

Endmembers were not generated using the maximum [*Chl-a*], [*SPM*] and a_{CDOM} in the water, firstly because concentrations higher than realistic in the area would deform the spectrum to a great extent. Secondly, creating endmembers based on the "highest" concentration is not possible: ultimate reflectance of a pure substance will remain (e.g., a spectrum with infinite SPM concentrations will provide the reflectance of sediment), which is not the wanted endmember. On the other hand, there is no problem if a pixel has reflectances somewhat higher than the highest SPM endmember, since this pixel would be unmixed with this high-SPM endmember anyhow. The situation would only increase the modelling error. Therefore high, but not too high concentrations were chosen to generate the endmembers. Endmembers were generated for pure water, for water with low concentrations (SPM 1 g m^3, Chl-a 1 mg m^3, CDOM 0.2 m^{-1}), high concentrations (SPM 100 g m^3, Chl-a 60 mg m^3, CDOM 3 m^{-1}), and mixtures between low and high concentrations (so one substance low and two high, or two low and one high) of the three substances, leading to a total of 9 endmembers (n = 9). Endmembers simulated with one or two high concentrations (for example high [*Chl-a*]) were referred to as endmembers dominated by that substance(s) (e.g.: the Chl-dominated endmember); the endmembers simulated with low or high concentrations for all the three substances were referred to as the low-concentrations or the high-concentrations endmember. Data from Pope and Fry (25) and Morel et al. (26) were used for absorption properties of pure water (a_w) and data from Buiteveld (27) were used for the scattering properties of pure water (b_w).

In an unconstrained unmixing method the abundances can have any value, while in a constrained method the abundances are non-negative (6) and in a fully constrained method also the sum of the abundances is one (7).

$$a \geq 0,\ b \geq 0,\ c \geq 0,\ \ldots.\ i \geq 0 \quad (6)$$

$$a + b + c + \ldots i = 1 \quad (7)$$

In land remote sensing the fully constrained method is used often because the total land-cover (e.g., in the example the total of grass and asphalt in a pixel) should be 100%. To detect water types the same unmixing method should be used. Negative abundances should not be possible,

since always at least pure (sea)water is present. Measured [*SPM*] higher than the one endmembers were based on are possible so that reflectances higher than the highest endmember could occur, abundances should also sum to one. However, allowing sums higher than one would lead to, for example, 5 times a low-SPM endmember instead of 1 time the high-SPM endmember, which implies that more water with low [*SPM*] would have a similar reflectance as water with high [*SPM*], which is clearly not true. Problems would also occur with CDOM and Chl-a that absorb light and therefore decrease the reflectance in higher concentrations. Higher abundances of for example the CDOM dominated endmember lead to higher total reflectances, while more CDOM dominated water should lead to lower reflectances. Eq. (4) is therefore enhanced with constraints in Eqs. (6) and (7).

RESULTS AND DISCUSSION

Water type modelling with HYDROPT

Three of the four SIOP sets listed for HYDROPT were found to lead to the lowest χ^2 values at most locations in the MERIS acquisitions (Figure 3). Water type 2, whose SIOP set was measured in the North Sea, was only detected at a small spot in the data of July 4th. Apparently this SIOP set was less suitable for the data in these two acquisitions, or subtle differences between MERIS and TriOS data made the SIOP set more suitable for TriOS than for MERIS data.

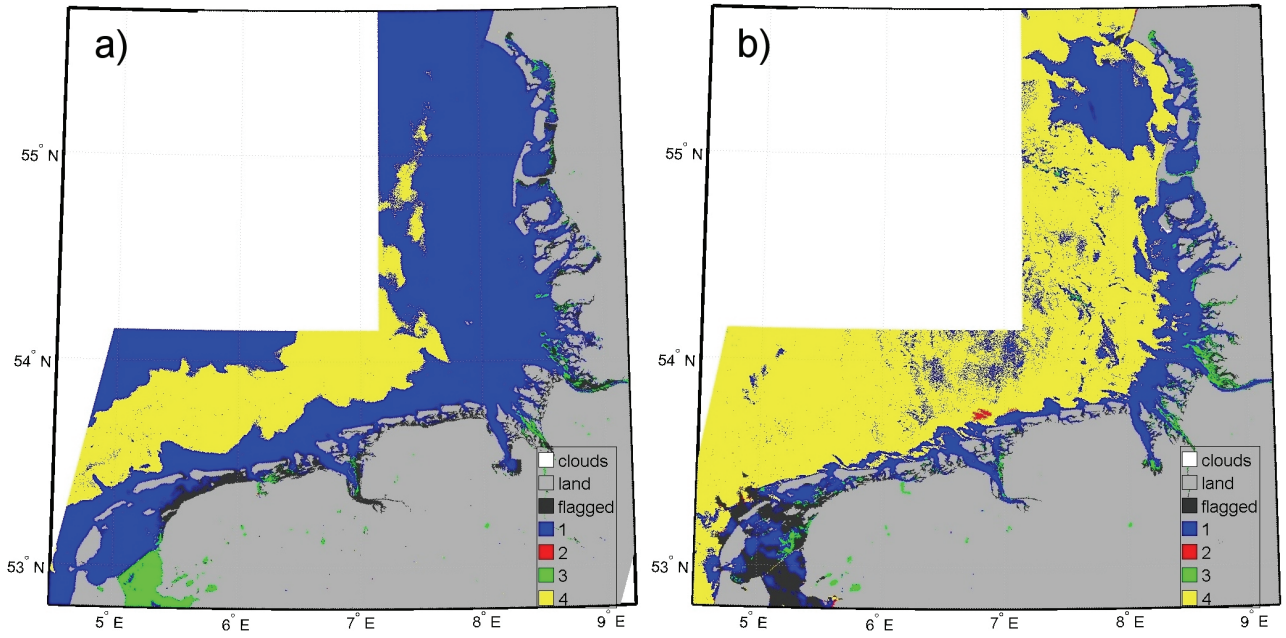

Figure 3: Water types modelled with HYDROPT. a) March 12th 2007, b) July 4th 2006. The colours indicate different SIOP sets.

In the Wadden Sea mainly water of type 1 was found, of which the SIOP set was measured at a location in the Dutch Wadden Sea. In the winter acquisition this water type was also found in a large area around the Wadden Sea and at some locations in the North Sea. This similarity between water in the Wadden Sea and water in large areas in the North Sea was thought to be due to resuspension. Both March 12th 2007 and July 4th had a moderate breeze that could cause resuspension, however, March 11th had been a windy day, while July 3rd also had just a moderate breeze. At March 12th the water could therefore contain more resuspended material than on July 4th. Also due to a lack of microphytobentos binding the sediment, resuspension is more prevalent in winter (28). Water type 3 was detected in the estuaries of the large rivers and Lake IJssel, which could logically be explained since the SIOP set of this water type had been measured in the outer estuary of the river Ems. Water type 4 was predominantly found in the North Sea. Although its SIOP set had been measured at a location in the Wadden Sea, it apparently contained material that was similar to material usually found in the North Sea. A relatively high salinity of 33 psu during sampling might explain the origin of the water of which the data of SIOP set 4 was obtained.

The dominant currents in the Wadden Sea are caused by the tide, moving in or out of the Wadden Sea through the channels between the islands, and by the rivers discharging water. The overall rest current in the Wadden Sea and German Bight is south-west to north-east. This pattern explains the pattern in water types seen: Wadden Sea water (type 1) flowing through the tidal channels to the North Sea and northward along the Danish coast, with a broader band of Wadden Sea water north of the Rivers Jade and Weser in the data of March 12th, which was acquired at low tide near the estuaries of these rivers. In the data of July 4th, which was acquired halfway during the outgoing tide near the estuaries of the large rivers, their discharge was less visible.

Water class modelling with endmembers

Water class modelling with endmembers showed clear distribution results (Figure 4). In both acquisitions, the endmember based on pure water was only found offshore in low abundances (not shown). The low-concentrations endmember was found in the relatively coastal areas of the North Sea, although in March more offshore (Figure 4a) than in July (Figure 4f). The other two endmembers that were predominant in the North Sea were the Chl-dominated and the Chl-CDOM-dominated endmembers. Note that high abundances of these endmembers provide information on the similarity between spectral shapes between these endmembers and the reflectance spectra in the North Sea, not on absolute concentrations. Chl-a, and CDOM as its degradation product, are likely more dominant in the North Sea than suspended matter, which settles out, while the shown area of the North Sea contains too much sediment for much similarity with the pure-water endmember.

In March the Chl-dominated endmember was found in one patch north of the Dutch islands (Figure 4b), in July, when phytoplankton concentrations are higher, it covered a larger area along the islands and in the discharge of the Weser and Elbe rivers (Figure 4g). In March, the Chl-CDOM-dominated endmember was only found in the same area as the Chl-dominated endmember (Figure 4c), while it covered a large area in the German Bight in July (Figure 4h).

In most of the Wadden Sea the Chl-SPM-dominated endmember gave the highest abundances. However, in March the abundances of this endmember were much higher than in July (Figure 4d and i). The SPM-dominated endmember gave, only in March, high abundances in the inner estuaries of the Jade and Dollard, as well as at a few locations in the Wadden Sea and at the north side of some Dutch and German islands (Figure 4e and j). In inland lakes and the River Weser the Chl-dominated endmember was predominant. In these acquisitions, the CDOM-dominated, SPM-CDOM-dominated and high-concentrations endmembers were only found with abundances lower than 0.1 (not shown).

The water classification with the endmember method visualises the higher influence of high (SPM) concentrations in March compared to July and the higher influence of chlorophyll, especially in the North Sea, in July.

Comparison of the two approaches

The water type detection with the inverse bio-optical model is a hard classifier, in that it showed strict boundaries between water types, while horizontal mixing is surely taking place. This is partly inherent to the method of selecting one SIOP set and therefore one water type per pixel, however, areas with altering pixels would be possible. The water class detection with endmembers is fuzzy, and is able to visualise the horizontal mixing between classes with decreasing versus increasing abundances. The derived water classes relate to concentrations, giving information on dominance and on “high” or “low” concentrations, and are useful for monitoring purposes. The method could also detect small patchiness in the Wadden Sea. On the other hand, the endmembers approach cannot provide precise information on concentrations of substances in the water, neither on the types of sediment, nor on pigments of CDOM in the water column. This is a consequence of applying a linear method to a non-linear system. Methods to circumvent this problem are the use of difference spectra as input (20) or unconstrained unmixing (19). However, these models are adapted for one substance and therefore lose their general application for water mass detection. The bio-optical model gives information on the SIOPs and therefore on the type of pigments, SPM or CDOM present, while it can derive the concentrations simultaneously with the water types (based on the total absorption and scattering from the LUT).

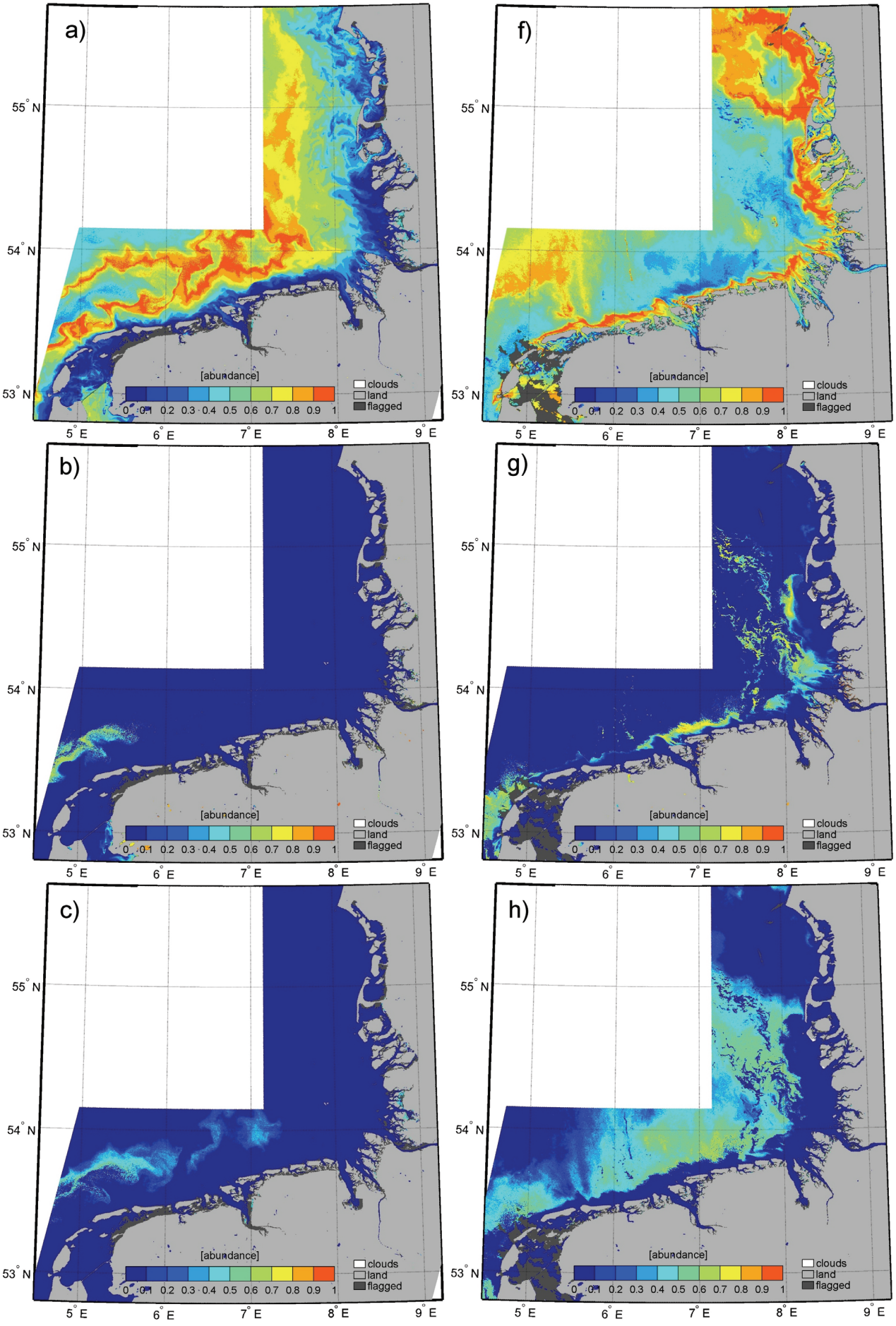
a)
b)
c)
f)
g)
h)
55° N
54° N
53° N
5° E
6° E
7° E
8° E
9° E
[abundance]
0 0.1 0.2 0.3 0.4 0.5 0.6 0.7 0.8 0.9 1
clouds
land
flagged

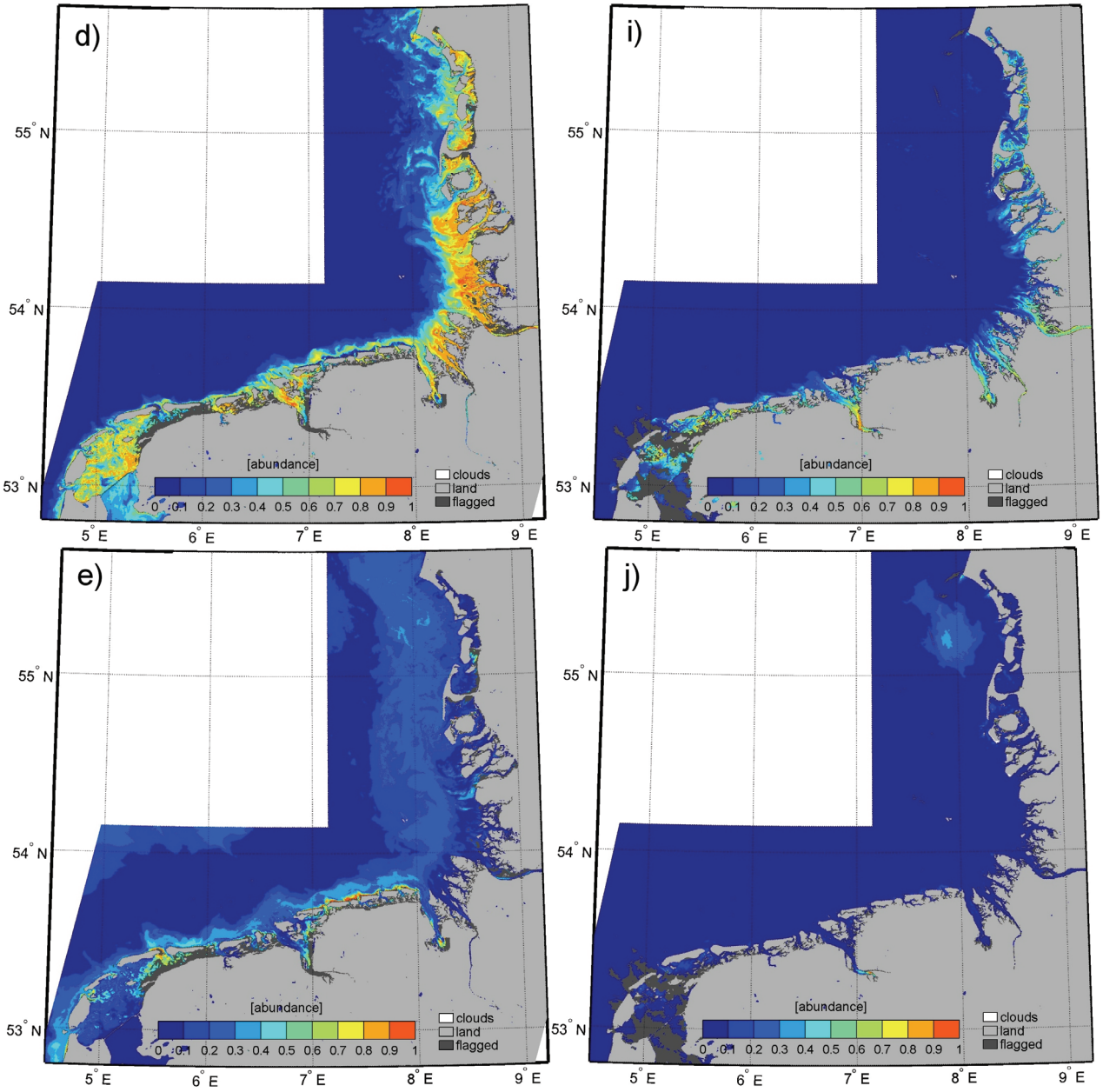

Figure 4: Water classes modelled with endmembers. Left panel a)-e): March 12th 2007, right panel f)-j): July 4th 2006. The colours represent the abundances of the endmembers: dark blue is low (0%) abundance, red is high (100%) abundance. Shown endmembers are: a) and f): low-concentrations endmember, b) and g): Chl-dominant, c) and h): Chl-CDOM-dominant, d) and i): Chl-SPM-dominant, e) and j): SPM-dominant.

CONCLUSIONS AND OUTLOOK

Both methods lead to results that could be explained with general knowledge on the water masses in the Wadden Sea and German Bight. The HYDROPT method shows a water type in the Wadden Sea that is different from the type in the German Bight. However, in a windy period in winter this Wadden Sea water type extends into the German Bight. This is thought to be caused by resuspension of bottom material, which is common in the Wadden Sea and extends to the German Bight after storm. Indeed, the Chl-SPM-dominated endmember has higher abundances in the same acquisition of March than in the acquisition of July. Generally, Chl-a and SPM are more dominant in the Wadden Sea than in the North Sea, where low concentrations prevail, according to the endmember method. Discharge from the large German rivers is visible in the results of HYDROPT, which finds another water type in the estuaries and northwards

Meanwhile, the techniques are different, leading to different but complimentary patterns. For example, the patch north of the Dutch islands classified with endmembers as Chl-dominated is not visible in the water type detection with HYDROPT. Apparently there is relatively more chlorophyll in that patch than in the surrounding water, while the phytoplankton is not of a different type. Similarities can strengthen the results of the two methods. The apparent influence of resuspension leading to water type 1 in the North Sea in March is visible with a low abundance for the SPM-dominated endmember. Also the patch west of the Danish islands (~55°N, 8°E) in the data of June is visible with both methods: the water is classified as type 1 while also this patch is influenced by the SPM-dominated endmember.

Although both methods lead to interesting results, the best tracing of water masses probably needs the combination of the two methods. For example, abundances of endmembers can be used to determine areas where certain SIOP sets of the bio-optical model would be most applicable, as in Moore et al. (21). However, this method assumes the SIOP to vary with the water classes. A combination of the results of the two methods assuming them to be complimentary can be interesting as well. The inverse bio-optical model misses the mixing, while the endmember model loses track of a water mass when, for example, CDOM degrades, or SPM sinks, while the water still moves in a horizontal direction. However, the water types of the inverse bio-optical model contain information on the type of material and therefore, in most cases, on the source, while the endmembers visualises the total influence of the substances in the water column on the colour of the water and therefore the horizontal mixing, degradation and sedimentation. With their specific possibilities the methods can supplement each other.

ACKNOWLEDGEMENTS

The captain and crew of the Royal Netherlands Institute for Sea Research R.V. *Navicula*, Kristi Uudeberg-Valdmets and Hamza el Abida are thanked for their help during the *in situ* campaigns. Raul Zurita-Milla is thanked for his advice on programming the unmixing model. Dr. Rainer Reuter is thanked for his suggestions on the endmember method at the EARSeL workshop. Reinold Pasterkamp provided the HYDROPT software libraries. Meteorological data at the day of image acquisition (wind speed and wind direction at the weather station at Lauwersoog (53.24˚N, 6.2˚E)), were extracted from the Royal Netherlands Meteorological Institute's database (www.knmi.nl/klimatologie/daggegevens/download.html). MERIS data was provided by the European Space Agency. This project was financed by NWO/SRON Programme Bureau Space Research, The Netherlands.

REFERENCES

1 Environment Directorate-General of the European Commission, 2000. Official Journal of the European Communities, OJ L 327. http://ec.europa.eu/environment/water/water-framework/index_en.html (688 kB pdf file, last access: 12 Jan 2010)

2 Zielinski O, J A Busch, A D Cembella, K L Daly, J Engelbrektsson, A K Hannides & H Schmidt, 2009. Detecting marine hazardous substances and organisms: sensors for pollutants, toxins, and pathogens. Ocean Science, 5: 329-349

3 Peeters E T H M, R J M Franken, E Jeppesen, B Moss, E Bécares, L-A Hansson, S Romo, T Kairesalo, E M Gross, E van Donk, T Nõges, K Irvine, R Kornijów & M Scheffer, 2009. Assessing ecological quality of shallow lakes: Does knowledge of transparency suffice? Basic and Applied Ecology, 10: 89-96

4 Hommersom A, S Peters, M R Wernand & J De Boer, 2009. Spatial and temporal variability in bio-optical properties of the Wadden Sea. Estuarine, Coastal and Shelf Sciences, 83: 360-370

5 Arnone R A, A M Wood & R W Gould, 2004. The evolution of optical water mass classification. Oceanography, 17: 14-15

6 Arnone R A, R Gould, W P Bissett, M Moline, O Schofield, G Chang & C Davis, 2004. Optical classification of watermasses using spectroscopy from space, Ocean Optics Conference XVII, Fremantle, Australia, CDROM, abstract 208, 1pp

7 Van Der Woerd H J & R Pasterkamp, 2008. HYDROPT: A fast and flexible method to retrieve chlorophyll-a from multispectral satellite observations of optically complex coastal waters. Remote Sensing of Environment, 112: 1795-1807

8 Pasterkamp R, H J Van Der Woerd, S W M Peters, M A Eleveld & J R Roberti, 2005. Simultaneous determination of suspended sediment and chlorophyll-a: validation for the North Sea in 2003. Proceedings of the Eighth International Conference on Remote Sensing for Marine and Coastal Environments, 17-19 May 2005, Halifax, Nova Scotia, Canada, 8 pp.

9 Santer R & F Zagolski, 2009. Algorithm Theoretical Basis Document ATBD - The MERIS level 1c. Issue 1, rev. 1, 6 Jan 2009: www.brockmann-consult.de/beam-wiki/download/attachments/13828113/ICOL_ATBD_1.1.pdf?version=1&modificationDate=1231230197000 (last access: 21 Feb 2010) 15 pp.

10 Doerffer R & H Schiller, 2008. Algorithm Theoretical Basis Document MERIS Case II ATBD-ATMO MERIS Regional Case 2 Water BEAM Extension Atmospheric Correction ATBD Issue 1, June 2008: www.brockmann-consult.de/beam-wiki/display/LAKES/ATBDs (last access: 21 Feb 2010) 42 pp

11 Doerffer R & M Peters, 2006. Algorithm Theoretical Basis Document MERIS Case II ATBD-ATMO - MERIS Regional Case 2 Water BEAM Extension. Flags ATBD. Version 1.1 16, November 2006: www.brockmann-consult.de/beam-wiki/display/LAKES/ATBDs (last access 21 Feb 2010) 5pp.

12 Mobley C D, 1994. Light and Water: Radiative Transfer in Natural Waters (Academic Press, New York) 592 pp

13 Dekker A, V Brando, J Anstee, T Pinnel, H Kuster, H Hoogenboom, S Pasterkamp, R Peters, O Vos & T Malthus, 2001. Imaging spectrometry of water. In: F van der Meer & S de Jong (eds.), Imaging Spectrometry: Basic Principles and Prospective Applications: Remote Sensing and Digital Image Processing (Boston: Dordrecht, Kluwer Academic Publishers IV) Chapter 11, pp. 307-359

14 Oubelkheir K, L A Clementson, I T Webster, P W Ford, A G Dekker, L C Radke & P Daniel, 2006. Using inherent optical properties to investigate biogeochemical dynamics in a tropical macrotidal coastal system. Journal of Geophysical Research-Oceans, 111, C07021, doi:10.1029/2005JC003113: 15 pp.

15 Brando V E, A G Dekker, Th Schroeder, Y J Park, L A Clementson, A Steven & D Blondeau-Patissier, 2008. Satellite retrieval of chlorophyll CDOM and NAP in optically complex waters using a semi-analytical inversion based on specific inherent optical properties. A case study for Great Barrier Reef coastal waters. Proceedings of the Ocean Optics Conference XIV (Italy) CDROM, 10 pp

16 Loisel H, X Mériaux, J-F Berthon & A Poteau, 2007. Investigation of the optical backscattering to scattering ratio of marine particles in relation to their biogeochemical composition in the eastern English Channel and southern North Sea. Limnology and Oceanography, 52: 739-752

17 Zibordi G, F Mélin & J-F Berthon, 2006. Comparison of SeaWiFS, MODIS and MERIS radiometric products at a coastal site. Geophysical Research Letters, 33, L06617, doi:10.1029/2006GL025778, 4pp.

18 Dowell M, J-F Berthon & G Zibordi, 2008. The identification of optically distinct water types at global and regional scales: implications for algorithm development and validation. Proceedings of the Ocean Optics conference XIV, Italy. CDROM. 1 pp

19 Tyler A N, E Svab, T Preston, M Présing & W A Kovács, 2005. Remote sensing of the water quality of shallow lakes: A mixture modelling approach to quantifying phytoplankton in water

characterized by high-suspended sediment. International Journal of Remote Sensing, 27, 1521-1537

20 Jianguang W, X Qing, L Qinhuo & Z Yi, 2005. Extraction of chlorophyll-a concentration based on spectral unmixing model using field hyperspectral data in Taihu Lake. Defence Technical Information Centre, OMB No. 0704-0188, 3 pp. Published in Chinese in Scientia Geographica 27, 92-97

21 Moore T S, J W Campbell & H Feng, 2001. A fuzzy logic classification scheme for selecting and blending satellite ocean color algorithms. IEEE Tranasactions on Geoscience and Remote Sensing, 39, 1764-1776

22 Gordon H R, O B Brown & M M Jacobs, 1975. Computed relationships between the inherent and apparent optical properties of a flat homogeneous ocean. Applied Optics, 14: 417-427

23 Jerlov NG, 1976. Marine Optics (Elsevier, Amsterdam, The Netherlands) 231 pp.

24 Morel A & L Prieur, 1977. Analysis of variations in ocean color. Limnology and Oceanography, 22: 709-222

25 Pope R M & E S Fry, 1997. Absorption spectrum (380–700 nm) of pure water. II. Integrating cavity measurements. *Applied Optics*, 36: 8710-8722

26 Morel A, B Gentili, H Claustre, M Babin, A Bricaud, J Ras & F Tièche, 2007. Optical properties of the ‘‘clearest’’ natural waters. Limnology and Oceanography, 52: 217-22

27 Buitenveld H, J H M Hakvoort & M Donze, 1994. The optical properties of pure water. Proceedings of the SPIE, 2258, 174-183

28 Colijn F & K S Dijkema, 1981. Species composition of benthic diatoms and distribution of chlorophyll *a* on an intertidal flat in the Dutch Wadden Sea. Marine Ecology-Progress Series, 4: 9-21